ISSN: 0975-833X

Available online at http://www.journalcra.com

International Journal of Current Research
Vol. 18, Issue, 10, pp. 38671-38679, October, 2026
DOI: https://doi.org/10.24941/ijcr.50977.10.2026

INTERNATIONAL JOURNAL OF CURRENT RESEARCH

RESEARCH ARTICLE

EXPERIMENTAL STUDY OF THE STEP-BY-STEP COMPENSATION OF THE REACTIVE POWER OF A THREE-PHASE ASYNCHRONOUS MOTOR UNDER AN UNBALANCED SUPPLY

Moustapha KEITA[1,3,4], Yacouba CAMARA[2*,3,4], Jean Ouèrè TOUPOUVOGUI[1,4], Kossoko Babatoundé Audace DIDAVI[1,4]

[1,3,4]Higher Institute of Technology, Department of Instrumentation and Physical Measurements, Mamou, Guinea
[2]Mamou Higher Institute of Technology, Department of Energy, Mamou, Guinea; [3]Laboratory of Teaching and Research in Applied Energy, Gamal AbdelNasser University of Conakry, Conakry, Guinea; [4]Laboratory of Research in Applied Sciences (LaReSA), Higher Institute of Technology of Mamou, Mamou, Guinea

ARTICLE INFO

Article History:
Received 24th July, 2026
Received in revised form
20th August, 2026
Accepted 15th September, 2026
Published online 30th October, 2026

Key words:
Asynchronous Machine, Reactive Compensation, Power factor, Joule Losses, Voltage Unbalance, Energy Efficiency.

***Corresponding author:**
Yacouba CAMARA

ABSTRACT

This experimental study presents the reactive power compensation of a 1,500 W three-phase asynchronous machine, conducted at the PROFORELEC laboratory of the Higher Institute of Technology of Mamou. The methodology comprises three phases: analytical modeling based on the power triangle, configuration of the experimental test bench, and real-time acquisition of electrical parameters using a METROL ME440 analyzer coupled with Python-based data processing. The progressive injection of capacitive power via a 2 kvar capacitor bank enabled the correction of the initially very low no-load power factor (cos φ between 0.12 and 0.18) to an optimal value of 0.97. Experimental results reveal a drastic reduction in reactive power (from 1,145–1,220 var to 45–90 var, representing a 92% to 96% decrease) and apparent power (from 1,155–1,238 VA to 130–180 VA). This reduction is accompanied by a significant decrease in drawn line currents and an 8.3% reduction in consumed active power (from 204 W to 187 W), attributable to lower Joule losses in the stator. The study thus confirms the significant value of capacitive compensation in optimizing the energy efficiency of inductive systems and preserving grid distribution capacity, even under conditions of severe voltage unbalance.

Copyright©2026, Moustapha KEITA et al. *This is an open access article distributed under the Creative Commons Attribution License, which permits unrestricted use, distribution, and reproduction in any medium, provided the original work is properly cited.*

Citation: ***Moustapha KEITA, Yacouba CAMARA, Jean Ouèrè TOUPOUVOGUI, Kossoko Babatoundé Audace DIDAVI,*** **2026.** "Experimental study of the step-by-step compensation of the reactive power of a three-phase asynchronous motor under an unbalanced supply*". International Journal of Current Research*, 18, (11), 38671-38679,.

INTRODUCTION

Reactive energy plays a fundamental role in the operation of alternative power grids [1], [2], [3],[4], [5], [6]. Unlike active energy, which corresponds to the power actually consumed and transformed into work or heat, reactive energy does not directly produce useful work. It is nevertheless essential for the operation of industrial electromagnetic equipment such as asynchronous motors, transformers, inductor coils, as well as certain static converters (variable speed drives, inverters) [7], [8]. In an alternating grid, reactive energy constantly oscillates between generation sources and inductive or capacitive loads. This energy is required to establish and maintain the magnetic fields necessary for the magnetization of electrical machines. Without this reactive energy, electromagnetic coupling in these devices would be impossible, which would cripple the majority of industrial electrical infrastructure [7],[8],[9],[10]. However, the transit of significant reactive power over power lines leads to several major disadvantages: increased Joule losses on the line, excessive voltage drops, decrease in active power transit capacity and oversizing of installations. The management and optimization of this energy is therefore crucial to ensure the stability and quality of the voltage on the grid [13]. An imbalance or lack of compensation can lead to additional operating costs, reduced efficiency or risks of overvoltage/undervoltage. This is why network operators and manufacturers deploy compensation solutions, such as capacitor banks, synchronous compensators or FACTS devices (such as the UPFC - Unified Power Flow Controller) [11],[8],[12], [13],[8], [14], [15], [16], [17],[18] In this context, a lack of reactive power degrades the power factor and forces the machine to absorb a larger line current to maintain its magnetic flux. Mastering this quantity makes it possible to optimize energy efficiency, avoid tariff penalties from electricity suppliers and free up capacity on the grid for new users[19], [20][21], [22],[23],[8], [24],[25],[26],[27],[28].

MATERIALS AND METHODS

Test Bench Materials

All the tests were carried out in the practical work room of the Laboratory of Electrical and Industrial Engineering of the Higher Institute of Technology of Mamou. The test bench consists of the following elements:

- Three-phase asynchronous machine: FLIPO RICHIR model, T3A-IE3 90 L4, from 1.5 kW at 50 Hz (1.8 kW at 60 Hz);
- Stepped capacitive bench: Maximum power of 2 kvar, allowing injection in steps of 0, %, 5, %, 10, %, 15, %, 20 % and 25 %;
- Network analyzer: METROL ME440 for real-time measurement of currents, voltages, powers (P, Q, S) and power factor;
- Protective equipment: Tetrapole thermomagnetic circuit breaker;
- Acquisition Environment: A data processing script developed in Python 3.x that runs in the Visual Studio Code environment.

The detailed nominal characteristics of the asynchronous machine under test are given in Table 1.

Table 1. The detailed nominal characteristics of the asynchronous machine

No	Parameter / Description	Value	Unit
1	Brand / Manufacturer	FLIPO RICHIR	-
2	Type / Model	T3A-IE3 90 L4	-
3	Serial Number	20220235701	-
4	Mounting Mode (IM)	B3	-
5	Ingress protection (IP)	IP 55	-
6	Rated Frequency	50 / 60	Hz
7	Rated power	1.5 / 1.8	kW
8	Rotational speed	1440 / 1730	r/min
9	Rated voltage	230/400 / 276/480	V
10	Rated Current	5.71/3.30	A
11	Pairing	Δ/Y	-
12	Power factor (cos φ)	0.77	-
13	EFF-IE3 efficiency (100%)	85.3	%
14	EFF-IE3 efficiency (75%)	85.3	%
15	EFF-IE3 Efficiency (50%)	83.1	%
16	Service (DUTY)	S1	-
17	Insulation class (INS)	F	-
18	Thermal Probe (PTC)	150	°C
19	Max. room temperature	47	°C
20	Coupling-side bearing (Brg DE)	6205 2RZ	-
21	Reverse Side Bearing (Brg NDE)	6205 2RZ	-
22	Reference Standard	IEC 60034	-
23	Mass / Weight	18	kg

Theoretical Modeling and Mathematical Formulation: Analytical modeling by establishing empirical equations governing the line current absorbed, the power factor (Cos φ), as well as the reactive powers (inductive of the machine and capacitive necessary for compensation) in accordance with the power triangle.

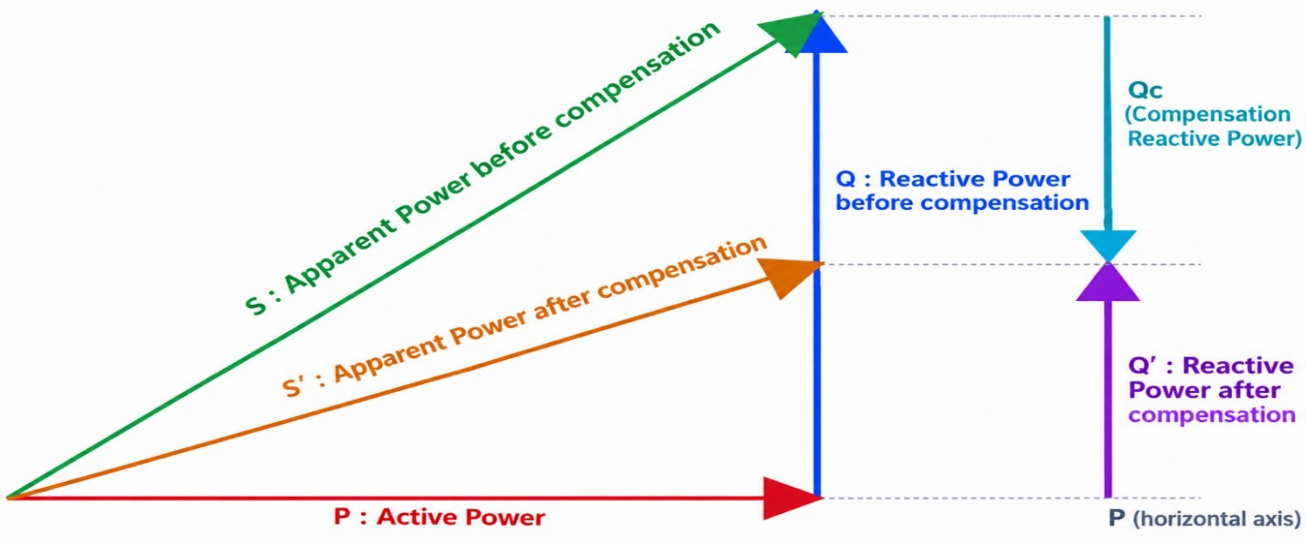


Figure 1. Power triangle

The three-phase apparent power S is given by:

$$S = \sqrt{3} * U_S * I_{abso} \quad (1)$$

The three-phase active (P) and reactive (Q) powers are expressed respectively by:

$$P = \sqrt{3} * U * I * \cos\varphi = P_A + P_B + P_C$$

$$P_T = P_A + P_B + P_C \quad (2)$$

Three-phase reactive power

$$Q = \sqrt{3} * U * I * \sin\varphi = Q_A + Q_B + Q_C$$

$$Q_T = Q_A + Q_B + Q_C \quad (3)$$

The power factor (PF) is written:

$$\mathrm{PF} = \frac{P_{abc}}{S_{abc}} = \cos\varphi \quad (4)$$

In the presence of unbalanced voltages, the apparent power is also expressed from the total active and reactive powers:

$$S = \sqrt{P^2 + Q^2}$$

$$I_{abso} = \frac{S}{\sqrt{3U_S}}$$

$$U_S = \sqrt{\frac{\sqrt{(U_{AB} + U_{BC} + U_{CA})}}{3}} \quad (5)$$

The average line current absorbed is estimated by:I_{abso}

$$I_{abso} = \frac{S}{\sqrt{3U_S}} = \frac{\sqrt{P_T^2 + Q_T^2}}{\sqrt{3U_S}} \quad (6)$$

Determination of the rate of unbalanced diet. In an electrical network, if the rate of imbalance exceeds 2 to 3%, it qualifies the imbalance. The voltages at the level of the three phases are, respectively: , and .$U_{AB} = 215{,}14\ V U_{BC} = 235{,}47\ V U_{CA} = 391{,}09\ V$

$$VUF_{NEMA(\%)} = \frac{max(U_{AB} - U_{MOY}, U_{BC} - U_{MOY}, U_{CA} - U_{MOY}) * 100}{U_{MOY}} \quad (7)$$

With

$$U_{moy} = \frac{U_{AB} + U_{BC} + U_{CA}}{3} \quad (8)$$

$$U_{moy} = \frac{215{,}14 + 235{,}47 + 391{,}09}{3} = 280.56\ \mathrm{V}$$

Theoretical Modeling and Mathematical Formulation: Analytical modeling by establishing empirical equations governing the line current absorbed, the power factor (Cos φ), as well as the reactive powers (inductive of the machine and capacitive necessary

for compensation) in accordance with the power triangle.A rate of 39.4% is sufficient proof of the imbalance of the network, exceeding 2 to 3% for a non-unbalanced network [29].

After compensation by capacitive power, the reactive power seen by the network becomes approximately: $Q_{injeter}$

$$Q_{reseau} = Q_{charge} - Q_{condensateur} \quad (9)$$

The compensating power required to change the power factor from cos to cos is classically estimated by the relationship:$\varphi_1 \varphi_2$

$$Q_{injeter} = P(\tan \varphi_1 - \tan \varphi_2) \quad (10)$$

The electrical loss due to the joule effect due to the three windings of the asynchronous resistor machine and crossed by a current is defined by:$R_s I_i$

$$P_{Joule} = (R_A * I_A^2) + (R_B * I_B^2) + (R_C * I_C^2) \quad (11)$$

Experimental setup and instrumentation: Before powering up, the test bench and the acquisition system were prepared.

•Design of electrical wiring diagrams in line with the study regimes chosen.

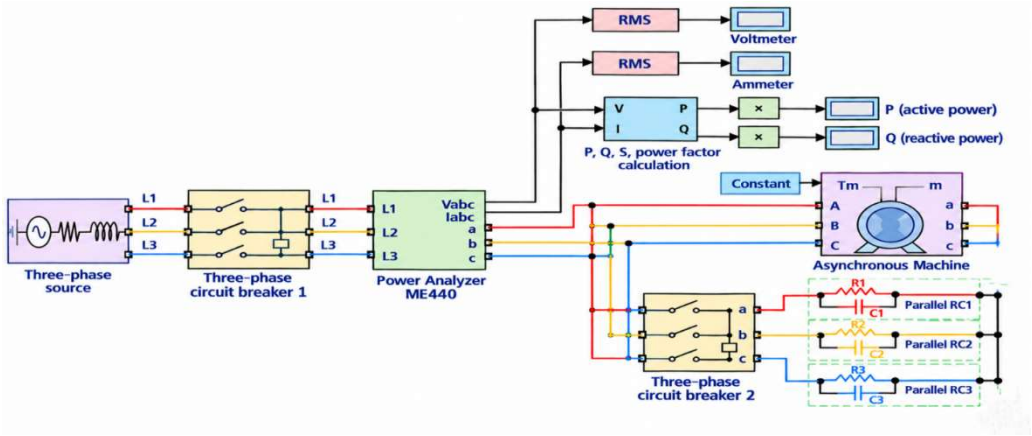


Figure 2. Electrical diagram of the assembly

- Configuration of the network analyzer (METROL ME440) according to the type of wiring of the machine. This configuration has been analyzed through the assembly shown in Figure 3.

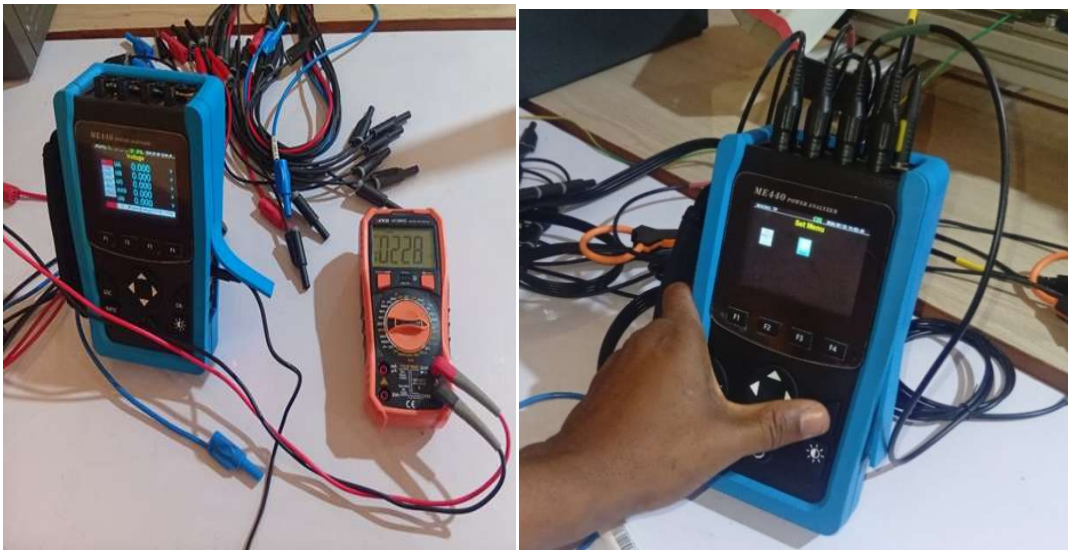


Figure 3. Configuring the Network Analyzer

•Preparation of the compensation device by wiring the capacitive reactive power injection device in accordance with the supply voltage and the coupling chosen, with a bench with a total capacitive reactive power of 2kvar.



Figure 4: Connecting the Capacitor Bank

RESULTS

The comparative analysis of the electrical data was conducted before and after the commissioning of the compensation. The signals were continuously retrieved and processed using the Python language. These analyses were carried out in two (2) steps, namely:

Statistical analysis before compensation: Table 2 summarizes the measurements made on the machine running no-load, under an unbalanced power supply and without capacitors.

Table 2: overall statistical summary of electrical measurements before compensation

Parameter / Quantity	Symbol	Unit	Minimum	Medium	Maximum	Standard deviation (σ)
UAB Compound Voltage	U_{AB}	V	212,27	214,81	216,82	1,02
UBC Compound Voltage	U_{BC}	V	230,46	234,57	236,67	1,59
UCA Compound Voltage	U_{CA}	V	387,08	390	392,41	1,3
Medium Single Voltage	U_{Avg}	V	277,37	279,79	281,75	1,02
Current Phase A	IA	A	2,44	2,54	2,63	0,04
Current Phase B	IB	A	3,08	3,16	3,26	0,03
Current Phase C	IC	A	2,67	2,83	2,98	0,07
Average Line Current	IAvg	A	2,79	2,84	2,9	0,02
Network Frequency	F	Hz	49,32	49,62	49,91	0,12
Power factor	PF	-	0,13	0,15	0,17	0,01
Total active power	P_{Sum}	W	149,36	181,33	204,87	14,95
Total reactive power	Q_{Sum}	var	1145,34	1182,06	1220,49	19,36
Total Apparent Power	S_{Sum}	VA	1155,2	1195,96	1237,41	20,46

When idle, the motor has an extremely low power factor of 0.15 on average. The average current absorbed is 2.84 A, consisting almost exclusively of magnetizing (reactive) current, which translates into an apparent power of 1195.96 VA for only 181.33 W of active power.

Statistical analysis with compensation: Table 3 shows the results after the capacitive bench has been engaged in successive steps. The results obtained are recorded in Table 3.

Table 3. Overall statistical summary - compensating trial

Parameter / Quantity	Symbol	Unit	Minimum	Medium	Maximum	Standard deviation (σ)
UAB Compound Voltage (Compensated)	UABc	V	212,43	217,72	223,18	3,08
UBC Compound Voltage (Compensated)	UBCc	V	228,05	232,12	234,25	1,39
UCA Compound Voltage (Compensated)	UCAc	V	385,73	389,95	393,40	1,57
Medium Single Voltage	UAvgc	V	276,83	279,93	282,65	1,26
Current Phase A	IAc	A	0,00	0,86	2,66	0,91
Current Phase B	IBc	A	0,75	1,56	3,01	0,75
Current Phase C	ICc	A	0,69	1,34	2,63	0,63
Average Line Current	IAvgc	A	0,48	1,25	2,74	0,76
Network Frequency	Fc	Hz	49,87	50,12	50,37	0,13
Overall Power Factor	PFc	-	0,12	0,56	0,98	0,34
Total active power	PSumc	W	115,06	154,76	187,10	18,33
Total reactive power	QSumc	var	32,74	420,00	1165,61	382,79
Total Apparent Power	SSumc	VA	131,23	474,82	1174,29	348,58

The effect of the compensation is clear: the overall power factor rises to a maximum of 0.98 (optimal level at t = 500 s}). On average, over the entire operation, including the transient phases, the average current drops to 1.25 A (compared to 2.84 A initially).

Presentation of results: The parameters studied are line currents, power factors, reactive, apparent and active power and these parameters are graphed with python 3.14.4 in the Visual studio code environment.

3.3.1 Currents absorbed by phase (IA for phase A, IB for phase B and IC for phase C)

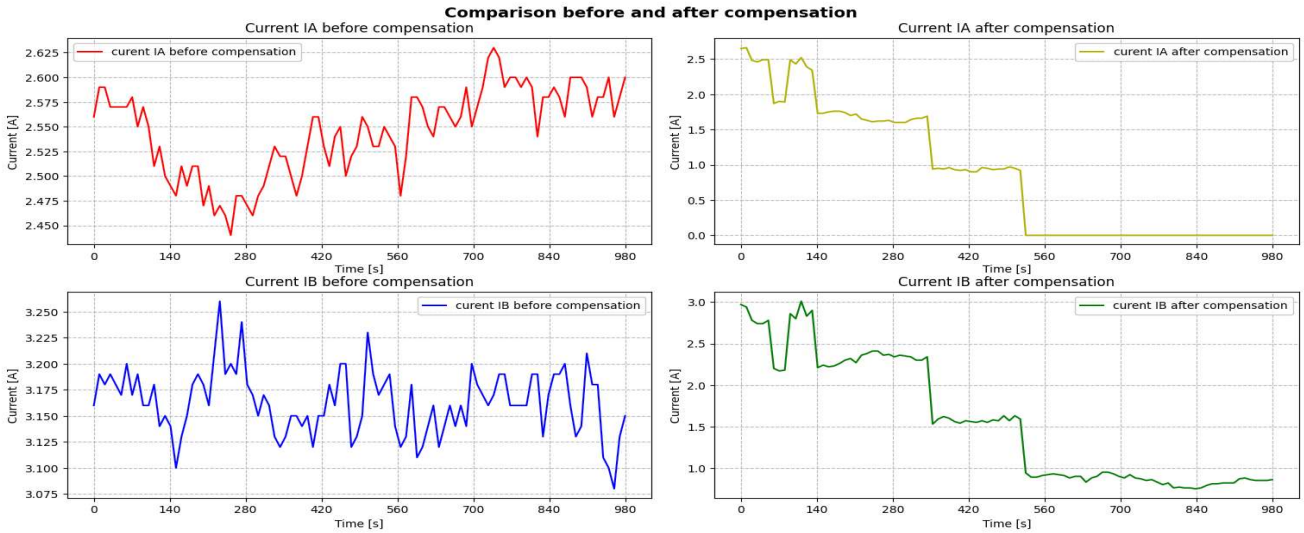


Figure 5. Pre- and post-compensation current curves of phase A and B

Before compensation, the line current of phase A varies approximately from 2.44 to 2.63 A and that of phase B from 3.08 to 3.26 A. After compensation, the currents decrease in stages. In phase B, the final current is close to 0.75–0.95 A, which reflects a significant reduction in the reactive component called to the grid. Zero current on phase A: around 480 s, *IA* drops exactly to zero, and the asynchronous machine runs at no load requiring only reactive current from the compensating bench.

3.3.2 Currents Absorbed by Phase (CI for Phase C) and Average Power Factor

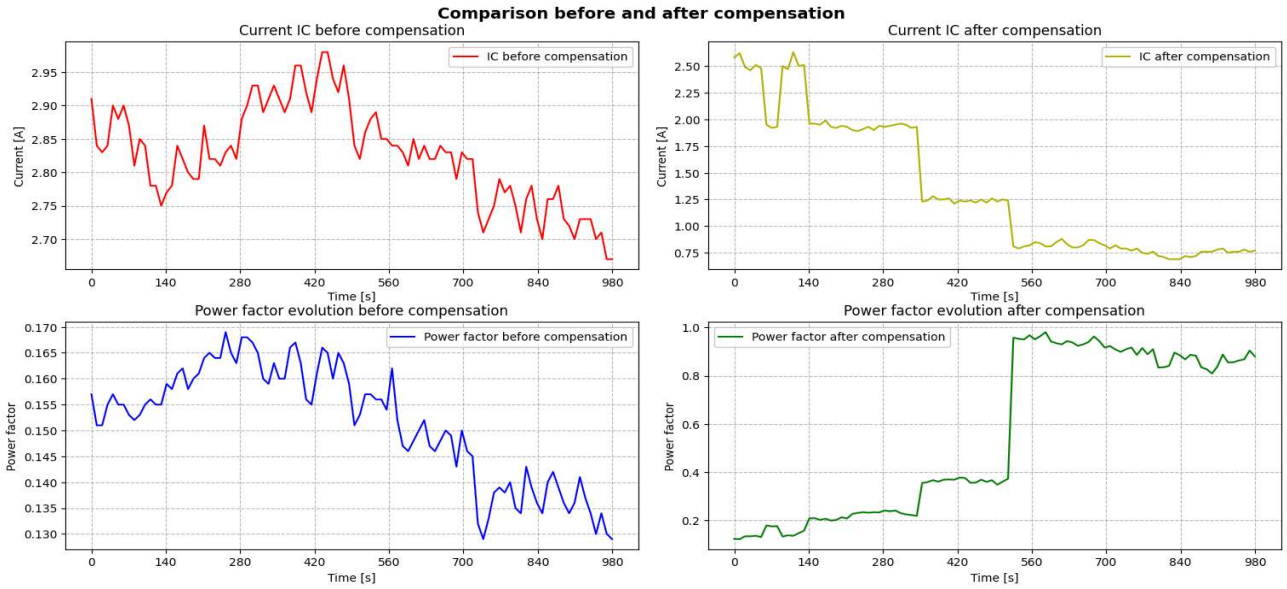


Figure 6. Phase C current and average power factors of phases A, B, and C

The current in phase C decreases from about 2.67–2.98 A before compensation to about 0.70–0.90 A at the last step. This decrease is consistent with the reduction in apparent power. The power factor before compensation is extremely low, generally between 0.13 and 0.17 because an asynchronous machine operates at no load, requiring a large part of magnetizing power (inductive load) and low active power. After compensation, the power factor improves in stages: about 0.12 to 0.18, then 0.20 to 0.25, then 0.35 to 0.38, before reaching approximately 0.95 after 480 s. The last interval nevertheless shows a temporary deterioration to about 0.82, followed by an increase to 0.97.

The average reactive and apparent power curves before and after phases A, B and C.

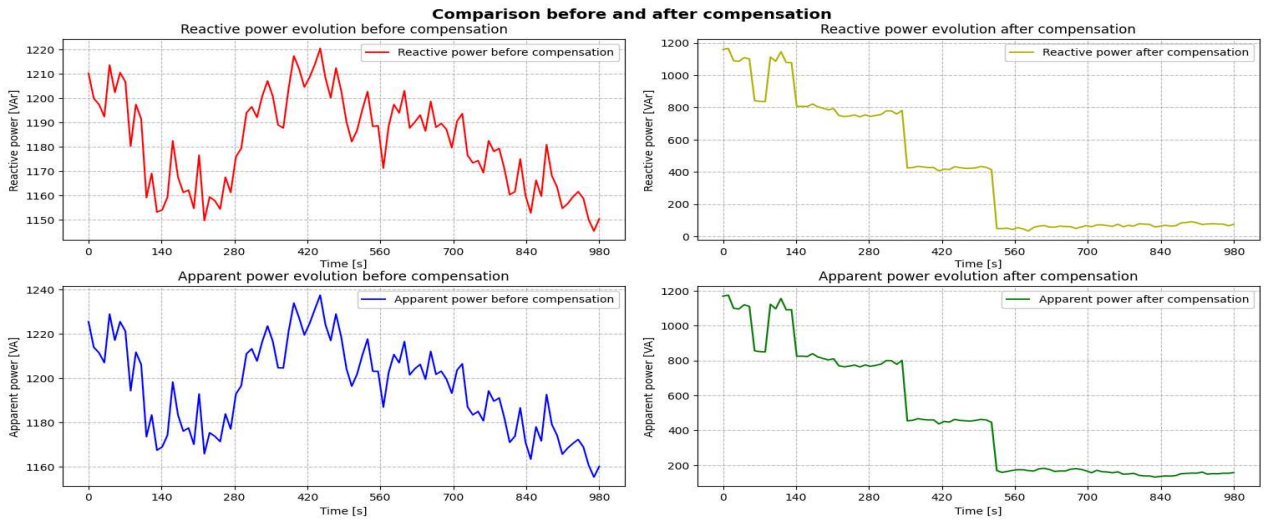


Figure 7. Reactive and effective power curves of phase A, B and C

Before compensation, the reactive power is approximately between 1145 and 1220 var, while the apparent power varies between 1155 and 1238 VA. The proximity between Q and S is consistent with the very low power factor, the load absorbs much more reactive power than active power because the machine is running idle. After the last step, Q becomes close to 45 to 90 var and S from 130 to 180 VA, we observe a compensation of the order of 92 to 96%, in the concern of overcompensation that we have stopped, otherwise the sign of Q would be negative and that of S of the order of 85 to 89%.

3.3.4 The average active power curves before and after phases A, B and C.

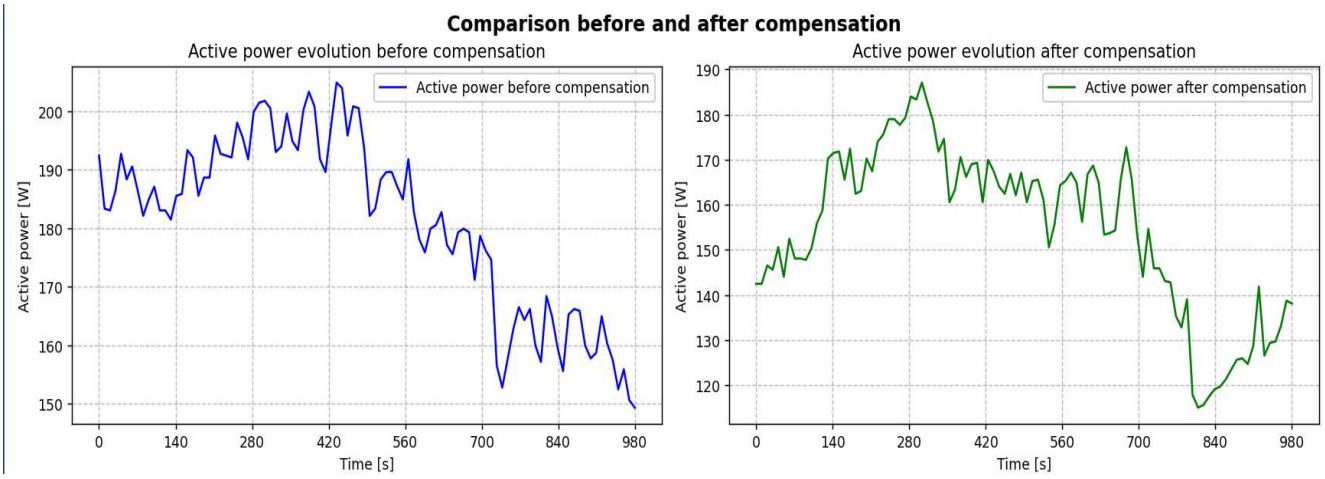


Figure 8: Average active power curves for phases A, B and C

Maximum active power 205 W before compensation and active power after compensation 187 W with a percentage decrease

$$\Delta_P = \frac{(P_{avant} - P_{apres}) * 100}{P_{avant}} \quad (12)$$

Pros $t = 700\ s,$ $P_{avant} = 204\ et\ P_{apres} = 187w$

$$\Delta_P = 100 * \frac{204 - 187}{204}$$

$$\Delta_P = 8,\%$$

DISCUSSION

Compensation analysis and reduction of active power: The reduction in the reactive power required from the grid is obvious: the overall average is down to 420 var, with a minimum of 32.74 var when the optimal levels are activated. This corresponds to an attenuation of the maximum reactive power of 92% to 96%.This decrease in current directly leads to a reduction in the losses due to the Joule effect in the stator windings. At t = 700 s}, the maximum active power consumed by the motor drops from 204 W (without compensation) to 187 W (with compensation). This reduction of about 8% in the active energy absorbed shows that by lightening the reactive load of the stator windings, the heating of the vacuum machine is significantly minimized.

Impact of the strong voltage imbalance: The calculated unbalance rate (39.4%) is exceptional for a conventional network. In standard industrial operation, such an imbalance induces a large inverse magnetic field that slows down the rotor and considerably increases losses. In the context of this manipulation, this extreme imbalance explains the major difference observed between the initial phase currents (IA = 2.54 A, IB = 3.16 A, CI = 2.83 A). Despite these pronounced asymmetries, the capacitor bank made it possible to optimize the overall power factor of the installation, validating the robustness of the principle of capacitive compensation even in highly disturbed networks.

Zero current phenomenon on phase A (IAc = 0 A): A remarkable result appears around t = 480 s} on the acquisition graphs: the current of phase A (IAc) cancels almost completely.

This behaviour can be explained by two combined factors:

- Near-perfect local compensation: At this capacitance level, the injected capacitive reactive current exactly compensates for the inductive magnetizing current of phase A.
- Asymmetrical power distribution: Under the effect of the strong voltage imbalance (UAB = 215 V, UCA = 391 V), phases B and C (subject to higher voltages) support all of the low active power required to maintain the engine's no-load rotation. Phase A is thus freed from any significant current transfer.

CONCLUSION

This experimental study highlighted the interest of capacitive compensation by steps on a three-phase asynchronous machine of 1.5 kW fed by a network whose unequilibrium rate is (VUF ≈ 39.4%). This compensation made it possible to:

- Reduction of line currents: The average current has been more than halved, relieving the congestion of line conductors and preventing thermal risks.
- Power factor optimization: The no-load cos φ increased from 0.15 to an optimal value of 0.97.
- Improved energy efficiency: Active power demand decreased by 8.3%, directly correlated with lower stator Joule losses.

The study confirms that step-by-step compensation remains an effective and cost-effective solution for cleaning up the electrical profile of inductive systems, even under severely degraded grid supply conditions.

REFERENCES

1. Hocine B. and B. Salah Eddine, "Compensation of Reactive Energy in Electricity Transmission Networks", Thesis, University of Ghardaïa, 2015. Accessed on: 11 March 2026. [Online]. Available at: https://dspace.univ-ghardaia.edu.dz/xmlui/handle/123456789/7100
2. Suli, S. Y. Öner, and İ. Şenol, "IE2 to IE4 Transition of Induction Motors for Sustainable Industry: Electromagnetic Performance, Loss Breakdown, Experimental Validation and Cost Analysis", *Appl. Sci.*, vol. 16, no. 13, p. 6799, Jan. 2026, doi: 10.3390/app16136799.
3. "Study of a 1k reactive energy compensation installation".
4. Abdulrahman Mohammed Galadima, "Reactive Power Compensation using STATCOM Based on Instantaneous Reactive Power Theory", *J. Syst. Eval. Miscellaneous. Eng.*, March 2025, doi: 10.70382/ajsede.v7i5.009.
5. "IEEE Standards Association," IEEE Standards Association. Accessed August 3, 2026. [Internet]. Available at: https://standards.ieee.org/ieee/1459/7578/
6. Joseph, T. N. F. T. N. Dianorré, O. Florence, N. Steyve, and M. P. Marcelin, "A Structured Probabilistic–AI Framework for Predictive Reliability Assessment and RUL Estimation of Asynchronous Rotating Machines", *ITEGAM-JETIA*, vol. 12, no. 60, pp. 685-703, juill. 2026, doi: 10.5935/jetia.v12i60.3969.
7. Tebani, W. "Optimal compensation of reactive energy in distribution networks", Thesis, 2018. Accessed on: 12 March 2026. [Internet]. Available at: http://dspace.univ-setif.dz:8888/jspui/handle/123456789/2090
8. Karim, P. M. F. P. Z. S. Ahmed, P. H. Samir, P. K. Mohamed, P. L. Fatiha, and U. de Saida, "Improving Power Flow in an Electrical Grid by the UPFC (Unified Power Flow Controller)."
9. Beugniez, A. T. Ghennam, B. François, E. M. Berkouk, and A. Et., "Centralized supervision of reactive power generation for a wind farm", *2007 Eur. Conf. Power Electron. Appl.*, 2007, doi: 10.1109/EPE.2007.4417485.

10. Brédard, F."Modeling and Control of a Variable Speed Wind Energy Conversion Chain Connected to the Grid and Using an Asynchronous Machine," Masters, Université du Québec à Rimouski, Rimouski, Quebec, 2014. Accessed on: March 12, 2026. [Online]. Available at: https://semaphore.uqar.ca/id/eprint/1089/
11. Belacheheb, K. "Contribution to the study of FACTS compensation systems in general, UPFC in particular, for the control of power transit in a transmission network", phdthesis, Université Henri Poincaré - Nancy 1, 2000. Accessed on: 20 November 2025. [Online]. Available at: https://hal.univ-lorraine.fr/tel-01746445
12. Faiz, J. G. Shahgholian, and M. Ehsan, "Stability analysis and simulation of a single-phase voltage source UPS inverter with two-stage cascade output filter", *Eur. Trans. Electr. Power*, vol. 18, no. 1, pp. 29-49, Jan. 2008, doi: 10.1002/etep.160.
13. "Doctoral thesis in Improvement of power flow in an electricity network by the UPFC (Unified Power Flow Controller)".
14. Rajper, M. A. Kumar, A. Qaimuddin, and F. Ullah, "Multi-Objective ABC Algorithm to Optimally Place UPFC and Its Parameter Settings for Transmission Efficiency Enhancement", in *IEEC 2023*, MDPI, Sept. 2023, p. 33. DOI: 10.3390/engproc2023046033.
15. Sen K. K.and E. J. Stacey, "UPFC-unified power flow controller: theory, modeling, and applications," *IEEE Trans. Power Deliv.*, vol. 13, no. 4, pp. 1453-1460, Oct. 1998, doi: 10.1109/61.714629.
16. Shahgholian, G. M. Mahdavian, M. Janghorbani, I. Eshaghpour, and E. Ganji, "Analysis and simulation of UPFC in electrical power system for power flow control", in *2017 14th International Conference on Electrical Engineering/Electronics, Computer, Telecommunications and Information Technology (ECTI-CON)*, IEEE, 2017, pp. 62-65. Accessed on: November 13, 2025. [Internet]. Available at: https://ieeexplore.ieee.org/abstract/document/8096173/
17. Mezaache, M."Contribution to the Study of the Optimal Choice of the Location of the UPFC Device in Electrical Networks Using One of the Artificial Methods".
18. Bouafia, A. J.-P. Gaubert, F. Krim, and A. Chaoui, "Unity Power Factor Operation of Three-Phase PWM Rectifier Based on Direct Power Control", *EUROCON 2007 - Int. Conf. On*, 2007, doi: 10.1109/EURCON.2007.4400552.
19. Lahdeb, M. A. Hellal, and S. Arif, "Metaheuristic Batch Hybridizations Applied to the Optimal Flow of Reactive Power", *Rev. Sci. Sci. The Engineer*, vol. 1, no 1, p. 59-66, 2010.
20. "Reactive Energy: Definition, Cost, and Compensation." Retrieved October 8, 2025. [Online]. Available at: https://entreprises.selectra.info/energie/electricite/compteurs/puissance/apparente/energie-reactive
21. Chang Y.-C. and R.-F. Chang, "Maximization of Transmission System Loadability with Optimal FACTS Installation Strategy," *J. Electr. Eng. Technol.*, vol. 8, no. 5, pp. 991-1001, Sept. 2013, doi: 10.5370/JEET.2013.8.5.991.
22. Kartobi, L. "Optimization of FACT synthesis by algorithms: Genetics and particle swarms for the control of power grids", PhD Thesis, Ecole Nationale Polytechnique, 2006. Accessed on: March 9, 2026. [Online]. Available at: https://www.pnst.cerist.dz/detail.php?id=69005
23. "Article THE UNIFIED POWFBFLOW CONTROLLER A NEW APPROACH TO POWER TRANSMISSION CONTROL.pdf".
24. Hussein, N.A. A.A. Eisa, H.M. Mahmoud, S.A. Shehata, and E.-S. A. Othman, "Interline power flow controller (IPFC) characterization in power systems", *Int. J. Eng. Technol.*, vol. 7, no. 3, p. 1656, August 2018, doi: 10.14419/ijet.v7i3.14894.
25. "Unified Feed Quality Conditioner - Overview | ScienceDirect Topics". Accessed on: 2026 Mar 9. [Internet]. Available at: https://www.sciencedirect.com/topics/engineering/unified-power-quality-conditioner
26. Graf, F.-R. "Real time application of an optimal power flow algorithm for reactive power allocation of the RWE energy control center", in *IEE Colloquium on International Practices in Reactive Power Control*, Apr 1993, pp. 7/1-7/4. Retrieved on: 11 March 2026. [Internet]. Available at: https://ieeexplore.ieee.org/document/231086
27. "Unified Power Quality Conditioner (UPQC)", in *Power Quality in Power Systems and Electrical Machines*, Academic Press, 2008, pp. 443-468. doi: 10.1016/B978-012369536-9.50012-7.
28. Sen K. K. and E. J. Stacey, "UPFC-unified power flow controller: theory, modeling, and applications," *IEEE Trans. Power Deliv.*, vol. 13, no. 4, pp. 1453-1460, 1998.
29. Singh, S. B.A. K. Singh, and P. Thakur, "Accurate performance assessment of IM with approximate current unbalance factor for NEMA definition," *2014 16th Int. Conf. Harmon. Qual. Power ICHQP*, 2014, doi: 10.1109/ICHQP.2014.6842805.

****